

Low-temperature specific heat of Li_xNbS_2 intercalation compounds

D. C. Dahn,* J. F. Carolan, and R. R. Haering

Department of Physics, University of British Columbia, Vancouver, British Columbia, Canada V6T 1W5

(Received 21 October 1985)

We report measurements of the low-temperature specific heat of Li_xNbS_2 , for $0 \leq x \leq 1$. Samples were prepared by intercalating lithium into NbS_2 in electrochemical cells. X-ray diffraction and electrochemical measurements show that staged phases exist for some values of x . The electronic specific heat of Li_xNbS_2 is consistent with complete charge transfer from the intercalated lithium to the bands of the NbS_2 host. The lattice specific heat also exhibits large variations as a function of x . A discussion of the data in terms of continuum-elasticity theory suggests that intercalation produces large changes in the elastic constant c_{44} .

I. INTRODUCTION

The layered transition-metal dichalcogenides (LTMD's) and their intercalation compounds are the subject of considerable current interest¹ because of their unusual physical properties and technological applications. Lithium intercalation compounds of the LTMD's are particularly interesting, because they are the basis of new high-performance rechargeable batteries.²

Intercalation of LTMD hosts with electron donors such as lithium generally leads to changes in the host's electronic properties. In many cases these can be understood in terms of charge transfer from the intercalant to the lowest empty states in the bands of the host.¹ In Li_xNbS_2 , as in many lithium-intercalated LTMD's, the lithium concentration can be continuously varied over much of the range between $x=0$ and $x=1$ without phase separation. This is not the case in most graphite intercalation compounds³ or in LTMD's intercalated with organic molecules.¹ The rigid-band charge transfer model implies that as we increase x in Li_xNbS_2 , the Fermi level will move up through the NbS_2 bands. Since the electronic specific heat depends on the density of states at the Fermi level, measurements of the specific heat as a function of x should allow us to map out the NbS_2 electronic density of states.

In addition to the changes in electronic properties, intercalation is expected to modify the phonon properties of the host, both by the addition of new modes and by modifying the interlayer forces. Measurements of the phonon specific heat are therefore also of interest.

In this paper we report specific-heat measurements on 12 Li_xNbS_2 samples with $0 \leq x \leq 1$, for temperatures between 2 and 20 K. The electronic specific heat is discussed in terms of charge transfer and compared with predictions based on a calculated band structure for NbS_2 .^{4,5} Lattice specific-heat results suggest a dramatic softening of the elastic constant c_{44} for $0 < x \leq 0.3$.

II. PREPARATION AND STRUCTURE OF Li_xNbS_2

The Li_xNbS_2 used in this work was prepared by intercalation of Li into NbS_2 in electrochemical cells. A brief

summary of the preparation procedure is given here; it has been described in more detail elsewhere.⁶ The first step was the preparation of NbS_2 by reaction of the elements in evacuated quartz ampoules. Powdered Nb and S were used, and sufficient excess sulfur was added to ensure a stoichiometric product.⁷ The sealed ampoules were slowly heated to 950°C and held there for three days, cooled to 750°C, and annealed there for one day, then quenched in cool water. The product was a free-flowing powder. X-ray powder diffraction measurements indicate that all our NbS_2 was in the $2H$ crystal phase. The hexagonal lattice parameters were $a=3.324 \pm 0.005$ Å and $c=11.96 \pm 0.01$ Å. These are in agreement with previously published values.⁷

The electrochemical cells used contained a lithium metal anode and a cathode consisting of NbS_2 powder bonded to a nickel substrate. They were similar to cells described in a previous paper,⁸ except that the cathodes were larger, typically containing 0.3 g of NbS_2 , and were passed between rollers to compact the layers of NbS_2 powder. Rolling the cathodes has been found to improve cathode utilization.

Intercalation of the Li_xNbS_2 samples used for specific-heat measurements was carried out by discharging cells to a preset voltage using a PAR model 173 potentiostat. Values of x in Li_xNbS_2 were determined coulometrically. The equilibrium voltages and x values for the specific-heat samples are shown in Fig. 1. The continuous lines in the figure are voltage versus x curves obtained by slow constant current discharge and charge of a test cell. The $V(x)$ behavior is in agreement with previous, less accurate measurements.⁹

Electrochemical and *in situ* x-ray measurements indicate that staging occurs in Li_xNbS_2 , as it does in Li_xNbSe_2 .⁸ By applying essentially the same techniques as in Ref. 8, we have found⁶ that for $x > 0.23$, Li_xNbS_2 has a stage-1 structure; that is, there is an equal concentration of Li in each interlayer gap. For x between approximately 0.11 and 0.19, there is a stage-2 phase. In stage 2, every second interlayer gap contains Li, while the intervening gaps are empty (or nearly so). That this phase is truly stage 2 is shown by the presence of (007) and (009)

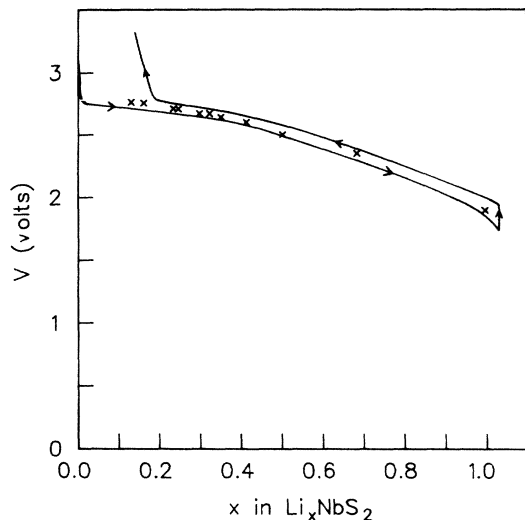


FIG. 1. Cell voltage as a function of x for $\text{Li}/\text{Li}_x\text{NbS}_2$ cells. The lines show the first discharge and the subsequent first charge of cell DD65. The charge and discharge were both at a rate of $\Delta x=1$ in 60 h. Also shown (\times) are the $V(x)$ values for each of the specific-heat samples.

Bragg peaks. In pristine NbS_2 and in the stage-1 intercalated compound, $(00l)$ reflections with l odd have a geometrical structure factor of zero. In the stage-2 compound, only one of the two interlayer gaps in the unit cell contains lithium and is expanded. The two layers in the unit cell are no longer equally spaced along the c axis, and

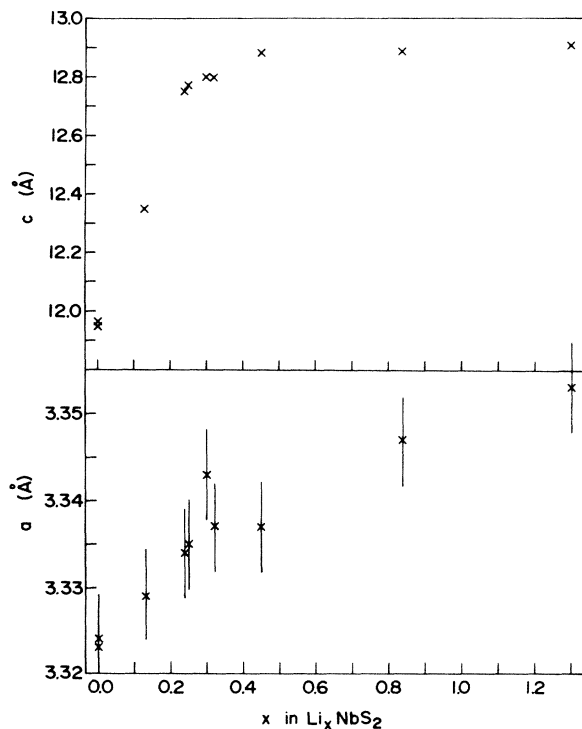


FIG. 2. Hexagonal lattice parameters a and c for Li_xNbS_2 . The unit cell is two layers high.

$(00l)$ peaks with l odd are allowed. Only (007) and (009) peaks have been observed, and intensity calculations⁶ show that the other $(00l)$ peaks with l odd should be relatively weak. In this material, staging is observed primarily through the expansion of the host lattice due to the fact that intercalated gaps expand, as the scattering power of lithium is very small. The stage-2 and stage-1 phases of Li_xNbS_2 both appear to have the same structure as $2H\text{-NbS}_2$ except for the addition of Li and the expansion of one or both of the interlayer gaps, respectively. This is an important point, since McEwan and Sienko¹⁰ report that Li_xNbS_2 prepared by high-temperature reaction forms in a $3R$ phase or a $2H\text{-}3R$ phase mixture for x between 0.01 and 0.13. Apparently, intercalating at room temperature avoids this. McEwan and Sienko also observed a (007) reflection in $2H\text{-Li}_x\text{NbS}_2$ for x between 0.13 and 0.17; they failed, however, to correctly identify it as being due to a stage-2 structure. There is also evidence for a disordered stage-3 phase near $x=0.08$, similar to that observed in Li_xNbSe_2 . It has not yet been investigated in detail.

Our measurements of the a and c axes of the 2-layer-high unit cell of Li_xNbS_2 are shown in Fig. 2. McEwan and Sienko have also measured a and c .¹⁰ When a positive systematic error in their x values¹¹ is allowed for, their results are in approximate agreement with ours.

III. SPECIFIC-HEAT MEASUREMENT PROCEDURE

Samples for specific-heat measurements were prepared by forming Li_xNbS_2 in electrochemical cells as described above. The cells were opened in an argon-filled glove box to recover the powder, which was then pressed into disk-shaped pellets using a steel die. Typical samples were 6 mm in diameter, about 2 mm thick, and weighed about 100 mg.

Heat-capacity measurements were made using the relaxation-time method.¹² As is usual in such experiments, the sample and its heater and thermometers were suspended from a temperature-regulated block in a vacuum chamber which was immersed in liquid helium. In our apparatus,⁶ the vacuum chamber may be plugged and removed from the rest of the cryostat. When detached, the chamber may be taken into the glove box for sample mounting. When the chamber is again attached to the cryostat, the plug is removed by means of a rod which runs up to the top of the apparatus. The samples were therefore never exposed to air. A microcomputer system was used for data acquisition and control. Because of the low thermal conductivity of our pressed pellet samples, the thermal decays were not single exponentials, and a data analysis procedure⁶ similar to that described in Appendix C of Ref. 12 has to be used. The absolute accuracy of the specific-heat measurement is estimated to be about $\pm 2\%$ in most cases.

IV. RESULTS

Low-temperature specific-heat measurements were made on NbS_2 , and eleven Li_xNbS_2 samples. Data for NbS_2 , $\text{Li}_{0.30}\text{NbS}_2$, and $\text{Li}_{0.50}\text{NbS}_2$ are shown in Fig. 3.

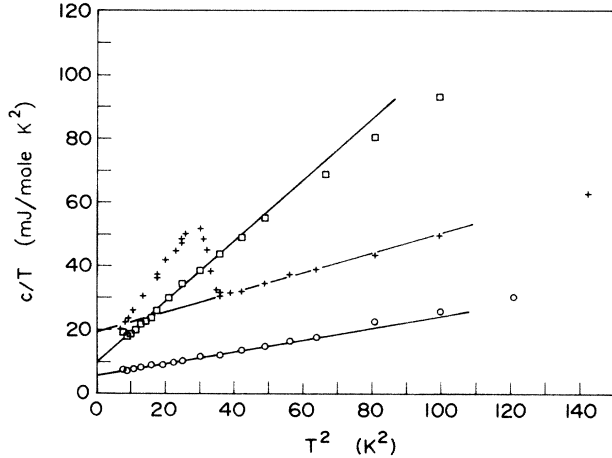


FIG. 3. Specific-heat data as a function of temperature for NbS_2 (+), $\text{Li}_{0.3}\text{NbS}_2$ (□), and $\text{Li}_{0.5}\text{NbS}_2$ (○). The lines are fits to Eq. (1).

The specific heat of a normal metal at sufficiently low temperature is expected to be of the form

$$c = \gamma T + \beta T^3, \quad (1)$$

where the linear and cubic terms are due to conduction electrons and phonons, respectively. The solid lines in Fig. 3 are least-squares fits to this equation.

In the case of NbS_2 , there is a large specific-heat anomaly due to the superconducting transition, which occurs between 5.5 and 6.0 K and is 50% complete at 5.7 K. Fitting the normal-state specific heat to (1) gives $\gamma = 19.3 \pm 1.5$ mJ/mole K^2 and $\beta = 0.31 \pm 0.04$ mJ/mole K^4 . This fit was constrained by the thermodynamic requirement that¹³

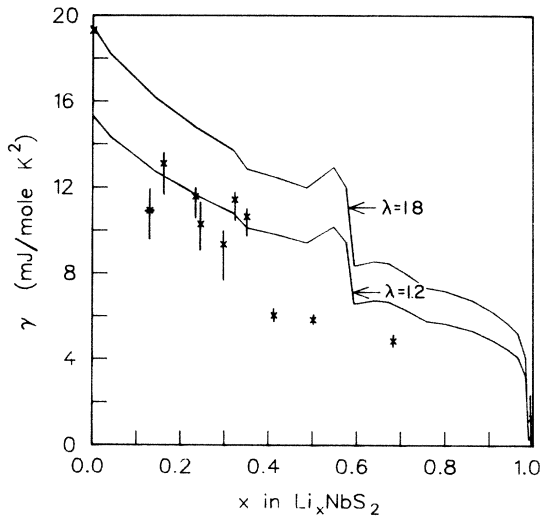


FIG. 4. Electronic specific-heat coefficient γ as a function of x in Li_xNbS_2 . The data are shown, together with the predictions of the rigid-band charge transfer calculation for two values of the electron-phonon coupling constant λ . The angular nature of the curve is the result of digitization of the graphical information in Ref. 5.

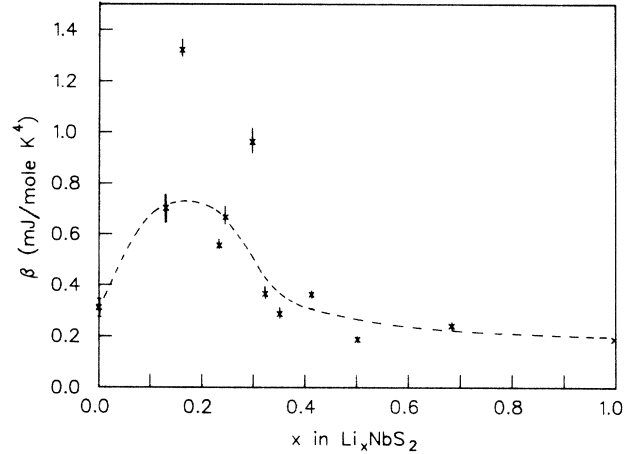


FIG. 5. Lattice specific-heat coefficient β as a function of x . The dashed line is intended only as a guide for the eye.

$$\int_0^{T_c} (c_s/T) dT = \int_0^{T_c} (c_N/T) dT, \quad (2)$$

where c_s and c_N are the specific heats in the superconducting and normal states, respectively.

The data for the other Li_xNbS_2 samples can also be fitted to Eq. (1), within experimental error. The coefficients γ and β are shown in Figs. 4 and 5, respectively. Only two of the intercalated samples were superconductors in the limited temperature range (> 2 K) studied; both the $\text{Li}_{0.23}\text{NbS}_2$ and $\text{Li}_{0.25}\text{NbS}_2$ samples had transitions at 3.1 K. Insufficient superconducting-state data are available to use Eq. (2) on these samples, however, so γ and β were determined by a fit to the normal state only.

V. ELECTRONIC SPECIFIC HEAT

Figure 4 shows the electronic specific-heat coefficient γ as a function of x . The results can be understood in terms of charge transfer from intercalated lithium into the NbS_2 bands. The band structure of NbS_2 has been calculated by Wexler and Wooley.⁴ Doran *et al.*⁵ used these results to calculate an electronic density of states. The bands are shown in Fig. 6 and the density of states for the dz^2 band in Fig. 7. The dz^2 band in NbS_2 is half filled, resulting in metallic behavior. The Fermi level lies on the side of a sharp peak in the density of states. Because of this, the calculated $N(\epsilon_F)$ should not be considered to be very precise. A slight change in ϵ_F would change $N(\epsilon_F)$ drastically. There is also a "shoulder" (van Hove singularity) in the density of states at $\epsilon - \epsilon_F = 0.27$ eV. This shoulder is due to the saddle point in the lower subband at Γ . Although the exact size and location of the shoulder depend on the details of the calculation, its existence does not.

Assuming rigid-band charge transfer (as discussed in the Introduction), intercalation progressively fills the dz^2 band, until it is completely full at $x = 1$. To calculate the electronic specific heat, we use the well-known relation

$$\gamma(x) = (1 + \lambda) \frac{\pi^2}{3} k_B^2 N(\epsilon_F(x)), \quad (3)$$

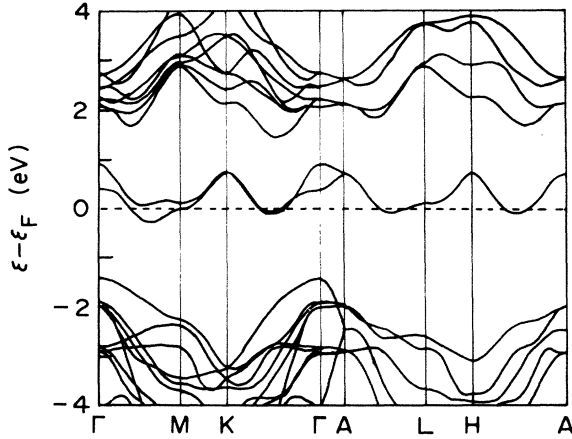


FIG. 6. Tight-binding fit to the layer method band structure of NbS_2 . A separate fit was used to determine the dz^2 band density of states. (From Ref. 5.)

where $N(\epsilon)$ is the molar electronic density of states (assumed in the rigid-band model to be independent of x), $\epsilon_F(x)$ is the Fermi energy of Li_xNbS_2 and λ is the electron-phonon coupling constant. Rigid-band filling implies that

$$x = \int_{\epsilon_F(0)}^{\epsilon_F(x)} N(\epsilon) d\epsilon, \quad (4)$$

which allows calculation of $\epsilon_F(x)$ and hence $N(\epsilon_F(x))$.

In order to calculate $\gamma(x)$ from Eqs. (3) and (4) we need, in principle, to know λ as a function of x . Given the lack of sufficient information to allow an independent determination of λ , we will make the approximation that it is constant. To assign a numerical value to λ we use the values of γ and $N(\epsilon_F)$ (Ref. 5) at $x=0$. These are 19.5 ± 1.5 mJ/mole K^2 and 2.94 states/eV-formula unit,

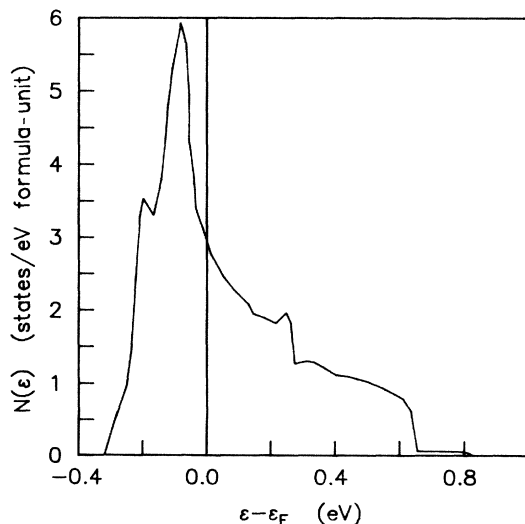


FIG. 7. dz^2 band density of states for NbS_2 (Ref. 5). The angular nature of the curve is the result of digitization of the graphical information in Ref. 5.

respectively, giving $\lambda=1.8$. This is in reasonable agreement with the values derived by Aoki *et al.*¹⁴ for NbS_2 .

The curve obtained by use of Eq. (3) and $\lambda=1.8$ is shown in Fig. 4, along with the data. A curve for $\lambda=1.2$ is also shown. The general features of the data and the calculated curves agree. Even in the context of rigid-band charge transfer, exact numerical agreement should not be expected, because of the approximate nature of the band calculations and the fact that variations in λ as a function of x are possible.

Several conclusions can be drawn from the data.

(i) γ tends to a value near zero at $x=1$. This supports the hypothesis of complete charge transfer, that is, each intercalated lithium atom donates one electron to the NbS_2 bands.

(ii) Use of the dz^2 bands of the NbS_2 host gives reasonable agreement with the Li_xNbS_2 data. There is no evidence that intercalation leads to either major changes in the dz^2 band or to band overlap in this material.

(iii) The shoulder in the specific-heat data at $x \approx 0.4$ indicates that this is the value of x for which the Fermi level of Li_xNbS_2 crosses the saddle point in the Li_xNbS_2 dz^2 band. If we assume a completely rigid band (that is, the Li_xNbS_2 dz^2 band is the same as the NbS_2 dz^2 band), this puts the following constraint on the density of states of NbS_2 :

$$\int_{\epsilon_F}^{\epsilon_S} N(\epsilon) d\epsilon = 0.4 \text{ states/(formula unit)}. \quad (5)$$

Here, ϵ_F and ϵ_S are the Fermi energy of NbS_2 and the energy of the saddle point, respectively. Note that this result does not depend on any assumptions concerning λ .

(iv) Two of the specific-heat samples ($x=0.13$ and 0.16) were stage 2. Staging changes the symmetry of the unit cell, and this will alter the host band structure. For instance, the two dz^2 subbands will no longer be degenerate on the top face of the Brillouin zone (the AHL plane). Stage-related changes in band structure are well known in graphite intercalation compounds,³ where the effects of staging must be allowed for if charge transfer models are to be used successfully. However, in stage-2 Li_xNbS_2 , the fact that γ agrees with the predictions of simple rigid-band charge transfer suggests that staging has little effect on $N(\epsilon_F)$. The specific heat in the stage-3 phase was not measured.

VI. PHONON SPECIFIC HEAT

The coefficient β of the T^3 term in the low-temperature specific heat is shown as a function of x in Fig. 5. Clearly, intercalation induces significant changes in the phonon spectrum. The Li_xNbS_2 samples with $0 < x < 0.4$ had β values greater than for NbS_2 , indicating a softer lattice. For higher values of x the lattice stiffens up again, and by $x=1$ the value of β is lower than in NbS_2 .

There are two main ways that intercalation can affect the vibrational properties of a NbS_2 sample. First, the addition of lithium atoms means the addition of new vibrational modes. Second, the original phonon modes of NbS_2 will be modified, because the presence of intercalated lithium will modify the interatomic forces, especially those between layers.

First consider the vibrational modes associated with a

single intercalated lithium atom. These are localized modes involving motion of the lithium atom and nearby sulfur and niobium atoms. However, since the lithium mass is much less than the mass of sulfur or niobium, we can make the approximation that the atoms surrounding the lithium are fixed and consider only the vibrations of the lithium about the center of its site. Lithium in Li_xNbS_2 is believed to lie in the octahedrally coordinated sites in the gap, as it does in Li_xTiS_2 .¹⁵ We can make a rough estimate of the restoring force constant for lithium motion normal to the layers from the "spring and plate" elastic model.¹⁶ In this model, intercalated lithium is described by springs which work against the original interlayer forces and push the layers apart. From the observed c -axis lattice expansion and an estimate¹⁷ of the elastic constant c_{33} of the NbS_2 host, we can estimate the strength of these "lithium springs." Attaching a lithium atom to the center of the "lithium spring" gives a restoring force of about 160 N/m, and a frequency $\omega_c \approx 10^{14} \text{ s}^{-1}$ ($=900 \text{ K}$). It is clear that this mode will not contribute significantly to the measured low-temperature specific heat.

A similar estimate may be made for lithium motion parallel to the layers. NMR studies of Li_xTiS_2 (Ref. 18) show that lithium moves between sites by thermally activated hopping over a 0.3-eV potential barrier. The situation in Li_xNbS_2 is probably similar. Assuming the sites are harmonic potential wells and using the barrier height above gives a frequency for in-plane motion of about $2 \times 10^{13} \text{ s}^{-1}$ ($=140 \text{ K}$). Again this will not contribute significantly to the low-temperature specific heat.

In the discussion above it was assumed that the lithium atom was on a site and that the only forces on it were those associated with localizing it on that site. When there are enough intercalated lithium atoms, however, they will interact with each other, and there may be lower frequency modes involving collective motion of the lithium. In principle, the situation is rather complicated, because of the staging phase transitions as well as the possibility of two-dimensional lithium ordering, which may occur in this system as it does in Li_xTaS_2 .¹⁹ These phase transitions may lead to soft modes. Some information on the strength of the lithium-lithium interaction is available from studies on the related Li_xTiS_2 system. Lattice gas model fits to electrochemical data¹⁶ used a repulsive nearest-neighbor interaction of 50 meV. This is much weaker than the 0.3-eV barrier between sites and suggests that it may be possible to ignore collective effects. In any case, the fact that the data fit a T^3 temperature dependence at low temperatures indicates that all low-lying modes have a linear (acoustic) dispersion relation.

Another way to discuss the results is to treat the intercalation compound as an anisotropic elastic continuum. In the low-temperature T^3 regime we are sensitive only to long-wavelength acoustic phonons and can interpret the results in terms of the macroscopic elastic constants of Li_xNbS_2 . To this end, it is useful to make an approximate calculation of β for NbS_2 . At low temperatures, the lattice specific heat (per mole) is given by βT^3 , where²⁰

$$\beta = \frac{2\pi^2}{5} k_B^4 V \frac{1}{(\hbar v)^3}, \quad (6)$$

V is the molar volume, and $1/v^3$ is the average over mode and direction of propagation of the inverse cubed sound velocity, that is,

$$\frac{1}{v^3} = \frac{1}{3} \sum_s \int \frac{d\Omega}{4\pi} \frac{1}{v_s(\hat{\mathbf{k}})^3}, \quad (7)$$

where v_s is the velocity of sound for mode s ($s=1, 2$, or 3) and direction of propagation along the unit vector $\hat{\mathbf{k}}$.

The sound velocities in a hexagonal crystal are functions only of the angle θ from the c axis, and are²¹

$$v_1(\theta) = (c_{11} \sin^2\theta + c_{33} \cos^2\theta + c_{44} - \{[(c_{11} - c_{44}) \sin^2\theta + (c_{44} - c_{33}) \cos^2\theta]^2 + (c_{13} + c_{44})^2 \sin^2\theta\}^{1/2})^{1/2} / (2\rho)^{1/2}, \quad (8a)$$

$$v_2(\theta) = [(c_{66} \sin^2\theta + c_{44} \cos^2\theta) / \rho]^{1/2}, \quad (8b)$$

$$v_3(\theta) = (c_{11} \sin^2\theta + c_{33} \cos^2\theta + c_{44} + \{[(c_{11} - c_{44}) \sin^2\theta + (c_{44} - c_{33}) \cos^2\theta]^2 + (c_{13} + c_{44})^2 \sin^2\theta\}^{1/2})^{1/2} / (2\rho)^{1/2}, \quad (8c)$$

where ρ is the density and the c_{ij} are the five independent elastic stiffness constants.

Mode 1 is a quasishear mode. At $\theta=0$ (propagation along the c axis), it becomes a pure shear wave, with atomic displacement in the plane of the layers. Since intralayer bonding forces are much stronger than interlayer forces, this acoustic wave involves essentially rigid layers vibrating as units, and is called a rigid-layer mode. At $\theta=\pi/2$, mode 1 is again a pure shear wave, now propagating in the basal plane with displacements along the c axis. In the limit of long wavelength, this is also a rigid-layer shear wave. The velocity of mode 1 at both $\theta=0$ and $\pi/2$ is $(c_{44}/\rho)^{1/2}$. c_{44} is the elastic constant associated with the rigid-layer shear. Mode 2 is a pure shear wave for all θ . At $\theta=0$ it is a rigid-layer mode degenerate with mode 1, and at $\theta=\pi/2$, its sound velocity is $(c_{66}/\rho)^{1/2}$. Mode 3 is a quasilongitudinal mode.

Equations (8) can be used to evaluate v and hence β , provided the elastic constants are known. To our knowledge, the elastic constants of NbS_2 have not been measured. The NbS_2 Raman results of McMullen and Irwin²² are not sufficient for the calculation of a complete set of elastic constants, although they do support the assumption that the elastic constants of NbS_2 are roughly the same as those of other related LTMD's. However, since the purpose of the calculation is primarily to identify which elastic constants are most important in determining the specific heat, approximate values will suffice. We will assume that the elastic constants of NbS_2 are close to those for NbSe_2 . A reasonable set of values for these is,²³ in units of 10^{10} N/m^2 ; $c_{11}=10.8$, $c_{33}=4.6$, $c_{44}=1.9$, $c_{66}=4.6$, and $c_{13} \approx 1$. The choice of NbSe_2 is not critical. Other related LTMD's with the $2H$ structure, such as TaS_2 and MoS_2 , have elastic constants reasonably close to these.

When β is evaluated using these elastic constants, $\rho=4.6 \text{ g/cm}^3$ for NbS_2 and Eqs. (6), (7), and (8), we get $\beta=0.22 \text{ mJ/mole K}^4$. The experimental value is 0.31 mJ/mole K^4 . This is reasonably good agreement, consid-

ering the calculations were made using the elastic constants of a different material. More important than the value of β is the fact that the rigid-layer shear modes make by far the largest contribution to β . Sixty percent of the calculated phonon specific heat is due to mode 1. This suggests that β in this system is controlled most strongly by c_{44} . Another way to see this is to calculate the derivatives $\partial\beta/\partial c_{ij}$. These are, in units of $10^{-15} \text{ m}^2\text{J/N mole K}^4$,

$$\begin{aligned} \frac{\partial\beta}{\partial c_{11}} &= -0.42, & \frac{\partial\beta}{\partial c_{33}} &= -1.5, & \frac{\partial\beta}{\partial c_{44}} &= -7.9, \\ \frac{\partial\beta}{\partial c_{66}} &= -1.5, & \frac{\partial\beta}{\partial c_{13}} &= +1.0. \end{aligned}$$

Since β depends most strongly on c_{44} and since c_{44} depends primarily on interlayer forces and should therefore be strongly affected by intercalation, we believe our Li_xNbS_2 data reflect the way c_{44} changes as a function of x . The only other elastic constant which depends mainly on interlayer forces is c_{33} ; this, however, has relatively little influence on β . In this interpretation, the high β values for the samples with $0 < x < 0.4$ indicate low values of c_{44} , relative to NbS_2 .

The reason why c_{44} is low for $0 < x < 0.4$ is not yet fully understood. As shown in Fig. 2, the c axis expands rapidly as a function of x in this composition range. As the layers separate due to intercalation, the interlayer shear forces appear to be weakened. As x is increased further, it apparently begins to be possible for shear to be transmitted from one NbS_2 layer to the next through the intervening layer of lithium. In addition to effects due to layer separation, staging and possibly lithium ordering may be involved.

Note that β , and therefore c_{44} , do not appear to be smoothly varying functions of x for the set of samples studied. In particular, the samples at $x=0.16$ and 0.30 have higher β values than other samples with similar x values. These two samples were both prepared from the same batch of NbS_2 powder, shortly after it was made. The other samples were prepared from NbS_2 powder that had been stored in air for at least one, and usually several months. There is also some preliminary evidence⁶ that the electrochemical properties of freshly prepared NbS_2 are slightly different from "aged" NbS_2 . The fact that NbS_2 powder in air smells of sulfur suggests a tentative explanation for the fact that samples made from fresh NbS_2 had a higher phonon specific heat. If the NbS_2 has lost sulfur, it will have excess Nb, which can intercalate between the layers and help bind them together, thus reducing β . Further work is underway to understand the effects of sample freshness and stoichiometry on the specific heat and electrochemical properties.

VII. CONCLUSION

X-ray diffraction measurements of the structure of electrochemically prepared Li_xNbS_2 were made, and stage-2 and -3 phases have been identified. The low-temperature specific heat of NbS_2 and 11 Li_xNbS_2 sam-

ples with $0 < x < 1$ has been measured. For all the samples, the normal-state specific heat could be described by $c = \gamma T + \beta T^3$ at sufficiently low temperatures, where the linear and cubic terms are due to electrons and phonons, respectively.

The electronic specific heat is consistent with complete charge transfer from the intercalated lithium to the dz^2 band of the NbS_2 host. The dependence of γ on x reflects the structure of the dz^2 band. In particular, a shoulder (Van Hove singularity) predicted by earlier band-structure calculations^{4,5} can be seen in the data, and its position has been determined. It would be interesting to see if the rigid-band charge transfer model can correctly predict the electronic specific heat of other lithium-intercalated layer compounds as well. In Li_xTiS_2 , for example, we would expect γ to increase as a function of x for small x , since the dz^2 band is initially empty or nearly empty. It may also be possible to pass over the peak in the dz^2 -band density of states.

Since the electronic specific heat is proportional to the density of states at the Fermi level, our data show that $N(\epsilon_F)$ as a function of x does not have any of the detailed structure that has been observed in the superconducting transition temperature T_c of Li_xNbS_2 .¹⁰ If the unusual behavior of T_c as a function of x reported by McEwan and Sienko is confirmed, it will therefore have to be explained in terms of intercalation-induced changes in the phonon spectra and electron-phonon coupling, rather than by the changes in $N(\epsilon_F)$ alone.

The phonon specific heat should reflect most strongly the elastic constant c_{44} of the material. The high β values observed for samples with $0 < x < 0.4$ indicate low values of c_{44} . It appears that c_{44} is also affected by the preparation and storage conditions of the NbS_2 used, and this point is being investigated further.

The intercalated lithium atoms may be thought of as interacting particles placed on a two-dimensional lattice of sites, with a fraction x of the sites full. One might expect unusual (and fundamentally interesting) vibrational modes in such a system.²⁴ The data, however, are consistent with the T^3 dependence of an ordinary three-dimensional anisotropic solid. We believe that the vibrational modes involving motion of the intercalant relative to the layers are probably at high frequencies *in this system*, because of the small mass of lithium and the depth of the potential well in which it sits. Layer compounds intercalated with heavier metals, for example, may behave completely differently.

ACKNOWLEDGMENTS

The authors would like to thank D. Li and J. Beis for assistance with the experimental work, B. Bergerson for stimulating discussions, and the Natural Sciences and Engineering Research Council for financial support. This work was performed as part of the Ph.D. requirements of one of the authors (D.C.D.), who would like to acknowledge the financial assistance of the Faculty of Graduate Studies and the Killam Trust.

- *Present address: Department of Physics, Dalhousie University, Halifax, Nova Scotia, Canada B3H 3J5.
- ¹A number of review articles and books dealing with the LTMD's and their intercalation compounds are available. Among the more recent are E. A. Marseglia, *Int. Rev. Phys. Chem.* **3**, 177 (1983); *Intercalation Chemistry*, edited by M. S. Whittingham and A. J. Jacobsen (Academic, New York, 1982); A. D. Yoffe, *Ann. Chim. Fr. Ser. 15*, **7**, 215 (1982); and the series *Physics and Chemistry of Materials with Layered Structures*, edited by F. Levy (Reidel, Dordrecht, 1976–79), Vols. 1–6.
- ²W. R. McKinnon and R. R. Haering, in *Modern Aspects of Electrochemistry*, edited by R. E. White, J. O'M Bockris, and B. E. Conway (Plenum, New York, 1983), p. 235, and references therein.
- ³M. S. Dresselhaus and G. Dresselhaus, *Adv. Phys.* **30**, 139 (1981).
- ⁴G. Wexler and A. M. Wooley, *J. Phys. C* **9**, 1185 (1976).
- ⁵N. J. Doran, B. Ricco, D. J. Titterton, and G. Wexler, *J. Phys. C* **11**, 685 (1978).
- ⁶D. C. Dahn, Ph.D. thesis, University of British Columbia, 1985.
- ⁷W. G. Fisher and M. J. Sienko, *Inorg. Chem.* **19**, 39 (1980).
- ⁸D. C. Dahn and R. R. Haering, *Solid State Commun.* **44**, 29 (1982).
- ⁹G. L. Holleck, F. S. Schuker, and S. B. Brummer, in *Proceedings of the Tenth Intersociety Energy Conversion Engineering Conference* (IEEE, New York, 1975), p. 1; B. DiPietro, M. Patriarca, and B. Scrosati, *Synthetic Metals* **5**, 1 (1982).
- ¹⁰C. S. McEwan and M. J. Sienko, *Rev. Chim. Minerale* **19**, 309 (1982); C. S. McEwan, Ph.D. thesis, Cornell University, 1983.
- ¹¹Some lithium was lost due to reaction with the quartz tubes used for sample preparation. C. S. McEwan, Ph.D. thesis, Cornell University, 1983, pp. 59,62.
- ¹²R. Bachmann *et al.*, *Rev. Sci. Instrum.* **43**, 205 (1972).
- ¹³M. W. Zemansky, *Heat and Thermodynamics* (McGraw-Hill, New York, 1957), p. 394.
- ¹⁴R. Aoki, S. Nakamura, and S. Wada, *Synthetic Metals* **6**, 193 (1983).
- ¹⁵J. R. Dahn *et al.*, *Can. J. Phys.* **58**, 207 (1980).
- ¹⁶J. R. Dahn, D. C. Dahn, and R. R. Haering, *Solid State Commun.* **42**, 179 (1982).
- ¹⁷We assume c_{33} is close to the value for the related material NbSe₂, where it has been measured (Ref. 23).
- ¹⁸R. L. Kleinberg, *J. Phys. Chem. Solids* **43**, 285 (1983).
- ¹⁹J. R. Dahn and W. R. McKinnon, *J. Phys. C* **17**, 4231 (1984).
- ²⁰N. W. Ashcroft and N. D. Mermin, *Solid State Physics* (Holt, Rinehart, and Winston, New York, 1976), Chap. 23.
- ²¹B. A. Auld, *Acoustic Fields and Waves in Solids*, (Wiley, New York, 1973), Vol. 1; see also N. Wakabayashi and R. M. Nicklow, in *Electrons and Phonons in Layered Crystal Structures*, edited by T. J. Weiting and M. Schluter (Reidel, Dordrecht, 1979), p. 409.
- ²²W. G. McMullen and J. C. Irwin, *Can. J. Phys.* **62**, 789 (1984).
- ²³J. L. Feldman, *J. Phys. Chem. Solids* **37**, 1141 (1976); **42**, 1029 (1981); *Phys. Rev. B* **25**, 7132 (1982); M. H. Jericho, A. M. Simpson, and R. F. Frindt, *ibid.* **22**, 4907 (1980).
- ²⁴For a study of a related one-dimensional system, see H. Von Lohneysen *et al.*, *Phys. Rev. Lett.* **46**, 1213 (1981).